Native spider silk as a biological optical fiber

N. Huby[1], V. Vié[1,] A. Renault[1], S. Beaufils[1], T. Lefèvre[2],F. Paquet-Mercier[2], M. Pézolet[2] and B. Bêche[1]

[1] Institute of Physics of Rennes UMR CNRS 6251, 263 avenue Général Leclerc, Rennes, France
[2] Centre de Recherche sur les Matériaux Avancés, Département de Chimie, Université Laval, Québec, Canada G1V 0A6

In this study we demonstrate the use of eco-friendly native spider silk as an efficient optical fiber in air, in highly bent fibers and in physiological liquid. We also integrated the silk filament in a photonic chip made of polymer microstructures fabricated by UV lithography. The molding process is non-destructive for silk and leads to an efficient micro-optical coupling between silk and synthetic optical structures. This optical performances, combined with the unique biocompatibility, bioresorbability, flexibility and tensile strength of silk filaments paves the way for new applications in biological media and for original biophotonic purposes.

Keywords: biopolymer, optical fiber, integrated optics, spider silk.

The development of optical fiber technology has increased the demand for new biological devices where light plays the role of sensor, actuator or laser beam carrier[1,2,3]. Implanted sensors are currently scarce, due to the challenges of miniaturization and biocompatibility. However, many examples of biological materials in nature show optimized structures and properties that are superior to synthetic materials[4,5].

Silk fibers produced by worms and spiders are among the most interesting materials for medical applications and for the development of new materials. They have a high degree of biocompatibility[6] and they are bioresorbable, ecologically friendly, and offer excellent mechanical properties[7,8,9]. Native silk fibers are used in textiles and surgical procedures but not yet in photonics.

Despite higher optical losses in plastic than in glass fiber, light weight, fracture tolerance and pliability are keys parameters explaining the interest in plastic fibers and their commercialization. Besides all these properties available for data transmission over short distances, fiber connections[10] and sensing applications[11], natural silk fiber combines unique advantages: it can be directly harvested from spiders or can potentially be obtained from renewable resources and in mild conditions (aqueous solvent, room temperature and moderate pressure), it exhibits a combination of strength and extensibility superior to any industrial material, and the natural production process leads to a diameter of 5 microns homogeneous over long distances. This is much thinner than conventional fibers, which creates a significant interest for minimally invasive medical applications involving light transmission, imaging or sensing in biological environments. Regenerated silkworm silk has been intensively studied and already applied in several fields[12,13]. Recent decades have seen the appearance of regenerated *Bombyx mori* silk-based devices[14,15,16,17], as either free-standing macroscopic elements such as lenses or microstructures patterned by thin-film processes[18,19,20].

In this letter, we demonstrate the efficient optical fiber behavior of pristine dragline silk from the spider *Nephila clavipes*. Spider silk was chosen because it has superior mechanical properties and homogeneity to any other natural and synthetic silk fibers[21]. By manipulating the silk fibers in air, the attenuation coefficient of the straight fiber was estimated about 10.5 dB/cm. Light propagation in a silk loop was also validated. Then, optical propagation was proved in silk fibers immersed in physiological liquid, confirming the potential and promising use in biological media. Finally, we demonstrated the integration of the pristine silk fiber into photonic chips and working optical hybrid devices containing synthetic polymers (photoresist) and natural silk fibers.

The investigation of the light propagation ability has been performed on a micro-optical bench (Fig. 1). Thanks to their long length, we developed a protocol to manipulate the silk fibers. The silk spinning process leads to fibers 5 µm in diameter over centimeters in length with a neat, smooth homogeneous surface as confirmed by Scanning Electron Microscopy (SEM) images (Fig. 1a). Sparse droplets visible on the silk fiber may be due to the presence of lipids, which can be removed

by immersion in an organic solvent[22]. During light propagation, these non-uniformities may be responsible for diffusion spots, although their influence is minimized by their presence only on one side of the fiber.

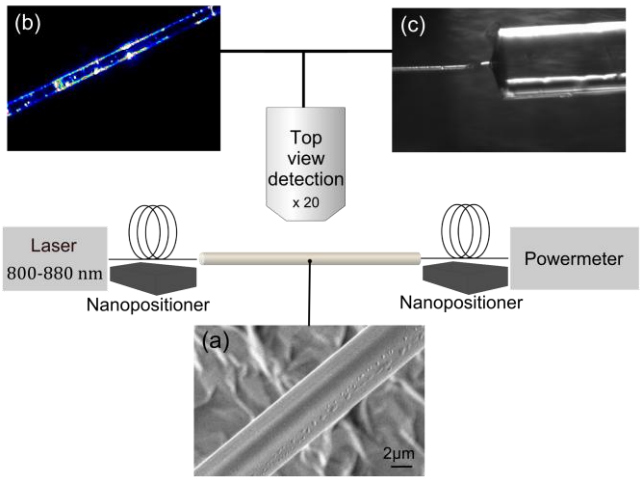

Figure 1. Set-up for light injection and detection in pristine spider silk fibers. a) SEM image of 5 µm diameter silk fiber. b) Top view of a micro-beam profile of a silk fiber during light injection. c) Top view imaging by a CCD camera of the microlensed fiber for light injection in silk.

Major ampullate (dragline) silk fibers from the orb-weaving spider *Nephila clavipes* came from adult female individuals collected in Florida and raised in the laboratory at 60% relative humidity and 24°C. The spiders were fed small crickets four times a week and 3 drops of 10% w/v glucose solution per week. The pristine silk fibers were forcibly reeled around test tubes from awake spiders at a linear speed of 1 cm/s. Without any particular treatment, silk fibers were positioned on an SiO_2 substrate, chosen to ensure the light confinement required for total internal reflection necessary for light propagation in optical fiber.

The refractive index of this dragline spider silk was previously determined to be about n_1=1.50[23], conferring a refractive index difference of Δn=0.05 with the lower SiO_2 cladding layer and Δn=0.5 with the upper air layer (n_2=1). Due to the dimension of the fiber, air acts as the main cladding layer since the contact area between SiO_2 and silk is small. The modal behavior of an optical fiber can be anticipated with the determination of the normalized frequency $V = \frac{2\pi a}{\lambda} \times NA$, where a is the core radius, λ the wavelength of the light in vacuum and NA the numerical aperture of the silk fiber $NA = \sqrt{(n_1^2 - n_2^2)} = 1.1$. For V values lower than 2.405, a single mode behavior is expected in optical fibers. The native silk fiber presents a value higher than 2.405 for visible and infrared light, conferring a multimode behavior. This is desirable for high intensity signal transmission.

A small radius of curvature (500 nm) for the microlensed fiber (*LovaLite*) is suitable for light focusing in the silk end facet. The transmitted power was detected at the output of the silk fiber by means of another fiber connected to a power meter (*Agilent* 81533). Both microlensed fibers were placed on *x-y-x* piezoelectric nanopositioners (*PI*) allowing 10 nm steps for accurate positioning. Injection was tested with infrared and red laser light. Top view detection was performed with either a micro beam profiler MBP (Fig 1b) or a CCD camera (Fig. 1c), using a 20× objective.

The optical losses in the fibers are described by the estimation of the attenuation coefficient α in dB/cm. For this purpose, the reliable cut-back method[24] based on the detection of the transmitted power through several lengths of sample was used here. The coefficient α in dB/cm can be calculated from the Beer-Lambert expression:

$$\alpha = \frac{10}{L_i - L_j} \times \log(\frac{P_j}{P_i}) \quad (1)$$

where P_j and P_i the output powers in nW detected at length L_j and L_i respectively, with $L_j > L_i$.
First, the output power P_1 of the silk fiber of known length L_1 is measured. The fiber is then cut to a shorter length L_2 without disturbing the injection silk facet and the corresponding output power P_2 is measured. This step is repeated at least 3 times per given silk sample. For each length, injection and detection are optimized with the nanopositioners to detect the maximum power. The length is then precisely measured on images recorded under an optical microscope.

Typical transmitted power data as a function of laser intensity (infrared broadband radiation λ=800 - 880 nm) are shown for fiber lengths ranging between 0.29 and 1.03 cm (Fig 2a). Applying Equation 2 to this data leads to the plot of the value of $10.\log(\frac{P_j}{P_i})$ as a function of $L_i - L_j$ (Fig. 2b). The linear fit for the four laser intensities leads to an attenuation coefficient of 10.5 ± 4.0 dB/cm. This value is two to three orders of magnitude higher than the synthetic polymer fibers[15], which have values of about 10^{-1} - 10^{-2} dB/cm at λ=800 nm, comparable with polymer integrated photonics waveguiding structures that show attenuation losses of a few dB/cm[25].

This difference may be first attributed to the fact that in synthetic fibers, the attenuation coefficient is obtained on optimized single mode fibers, for instance on doped polymers[26]. Here, the silk fibers are multimode and the measurements are performed on as-extracted material. A second reason could be attributed to the intrinsic structure of the silk. Studies are underway to correlate the optical and structural properties.

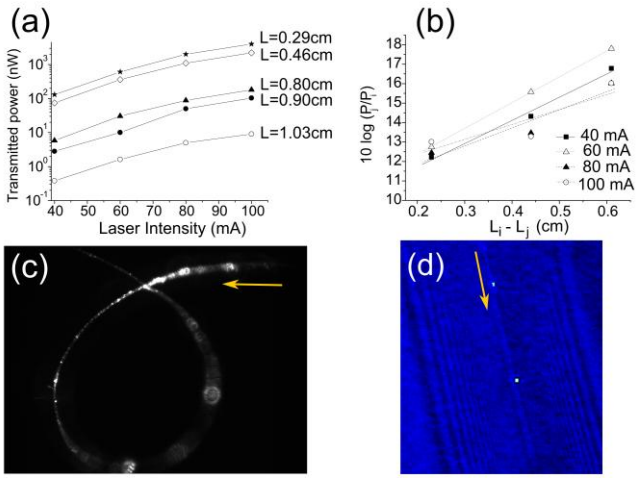

Figure 2. Optical results obtained for spider silk fibers manipulated in different configurations. a) Transmitted power as a function of laser intensity (λ=800 - 880 nm) for several lengths of straight silk sample. b) Value of 10 log (P_j/P_i) as a function of (L_i-L_j) measured for several laser intensities. Symbols correspond to experimental values and lines to linear fits. c) CCD top-view of a silk-loop with a diameter of 350 microns during light injection. The arrow indicates the direction of light d) MBP top-view of the light propagation in a silk sample immersed in physiological liquid.

Several configurations of natural silk fibers have been verified and their performance is being studied further. First, light has been propagated in a silk fiber loop with a 175 µm radius (Fig. 2c). The flexibility of this material is of great interest for flexible structures. The transmission of light in the silk fibers in a biological medium is of fundamental interest and practical relevance. The top view of immersed silk during light injection following the same injection procedure as previously described for the experiments in air has been recorded (Fig. 2d). The light spots along the silk fiber demonstrate the efficient propagation until the end of the fiber, including when the fiber is dipped in an aqueous medium.

To broaden the applications of spider silk, for example for uses in integrated sensors, the fiber has been integrated with a photonic chip. The silk filament is embedded in a SU8 photoresist during a lithography process that creates planar microstructures on a Si/SiO_2 substrate.

First, a drop of photoresist was deposited on the Si/SiO_2 substrate and the silk sample was deposited on top of it. It is spun at 3000 rpm for 30 seconds and baked on a hot plate (1 min at 65°C and 2 min at 95°C) to remove the undesirable solvents. The glass mask with designed microstructures such as waveguides and photon reservoir-disks was then judiciously positioned. After UV exposure, the substrate was immersed for 2 minutes in SU8 developer to selectively remove the non-exposed photoresist. A last baking step (1 min at 65°C and 2 min at 95°C) was applied to cross-link the polymer.

The process is visible on SEM images (Fig. 3a). The SU8 microstructures consist of 9 µm thick reservoir-disks (RD) connected to 6 µm wide waveguides. The 1.25 mm-long silk fiber has been positioned to connect RD1 and RD2. Image enlargement (Fig. 3b) confirms that the process is not destructive for the fiber as the diameter is still uniform and the surface is smooth with little sub-micronic residual photoresist. The silk appears as a bridge surrounded by air and sustained by the SU8 RD. For optical investigations, light is launched in the SU8 waveguide and propagates to the RD where light is confined on the edges, which is exploited for optical coupling to the silk (Fig 3c). Light scatters along the silk fiber, demonstrating that an efficient optical coupling takes place from RD1 to the native silk. Light appears confined at the RD2 edges, attesting to a second efficient coupling from the silk to the SU8 microstructure.

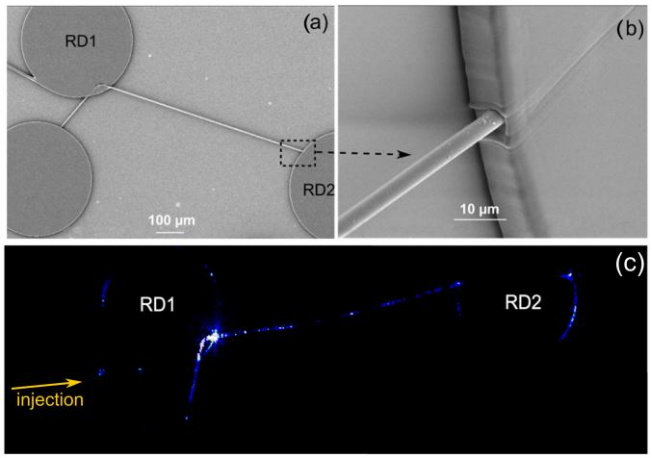

Figure 3. A pristine silk fiber integrated on a photonic chip. a) SEM image of the hybrid photonic chip based on silk fiber and SU8 microstructures depicting the silk fiber connecting 2 reservoir-disks RD1 and RD2. b) SEM close view of the silk embedded in the photoresist. c) MBP top view of the hybrid photonic chip based on silk fiber and SU8 microstructures. Light is injected in the waveguide connected to RD1.

These results describe the use of pristine spider silk fiber as an efficient optical fiber in air, in bent configurations, in biological media and in an integrated photonic chip. The remarkable mechanical properties of the spider silk allow manipulation for optical investigation. Optical losses of 10.5 dB/cm are appropriate for the applications designed to incorporate this unique fiber. These original data are very promising for biophotonic applications where light propagation and/or sensing in biocompatible media is required.

Silk may therefore represent a promising material for future optical applications in a sustainable society since it exhibits numerous advantages (biocompatibility, bioresorbability, biodegradability, flexibility and tensile resistance) and will most probably have a lower ecological footprint than synthetic polymers.

This work was supported by the Centre National de la Recherche Scientifique CNRS of France and by the Natural Sciences and Engineering Research Council (NSERC) of Canada and the Fonds de recherche du Québec – Nature et technologies (FRQ-NT).

[1] G. Boisdé and A. Harler, Artech House, Boston (1996).

[2] S. Goel, J.N. McMullin, H. Qiao and A. Grundmann, Review of Scientific Instruments **74**, 4145-4149 (2003).

[3] V. Svirin, V. Sokolov and T. Solovieva, Proceedings of SPIE **5116**, 322-333 (2003).

[4] R. Cattaneo-Vietti, G. Bavestrello, C. Cerrano, M. Sara, U. Benatti, M. Giovine and E. Gaino, Nature **383**, 397-398 (1996).

[5] V.C. Sundar, A.D. Yablon, J.L. Grazul, M. Ilan and J. Aizenberg, Nature **424**, 899-900 (2003).

[6] C. Allmeling, A. Jokuszies, K. Reimers, S. Kall, and P.M. Vogt, J. Cell. Mol. Med. **10**, 770-777 (2006).

[7] J.M. Gosline, M.E. DeMont and M.W. Denny, Endeavour **10**, 37–43 (1986).

[8] M. Heim, D. Keerl, and T. Scheibel, Angew. Chem. Int. **48**, 3584 – 3596 (2009).

[9] F. Vollrath and D.P. Knight, Nature **410**, 541 (2001).

[10] O. Ziemann, J. Krauser, P.E. Daum and W. Daum, Polymer Optical Fiber Handbook, Springer, Berlin (2008).

[11] K. Peters, Smart Mater. Struct. **20**, 013002 (2011).

[12] H. Tao, D.L. Kaplan and F.G. Omenetto, Adv. Mat. **24**, 2824-2837 (2012).

[13] S. Ghost, S.T. Parker, X. Wang, D.L. Kaplan and J.A. Lewis, Adv. Funct. Mater. **18**, 1883-1889 (2008).

[14] C. Müller, M. Hamedi, R. Karlsson, R. Jansson, R. Marcilla, M. Hedhammar and O. Inganäs, Adv. Mater. **23**, 898-901 (2011).

[15] H. Tao, J.J. Amsden, A.C. Strikwerda, K. Fan, D.L. Kaplan, X. Zhang, R. Averitt and F.G. Omenetto, *Adv*. Mater. **22**, 3527-3531 (2010).

[16] P. Domachuk, H. Perry, J.J. Amsden, D.L. Kaplan and F.G. Omenetto, Appl. Phys. Lett. **95**, 253702 (2009).

[17] J.J. Amsden, H. Perry, S.V. Boriskina, A. Gopinath, D.L. Kaplan, L. Dal Negro and F.G. Omenetto Opt. Expr. **17**, 21271 (2012).

[18] B.D. Lawrence, M. Cronin-Golomb, I. Georgakoudi, D.L. Kaplan and F.G. Omenetto, Biomacromolec. **9**, 1214-1220 (2008).

[19] S.T. Parker, P. Domachuk, J. Amsden, J. Bressner, J.A. Lewis, D.L. Kaplan and F.G. Omenetto, Adv. Mater. **21**, 2411-2415 (2009).

[20] R. Capelli, J.J. Amsden, G. Generali, S. Toffanin, V. Benfenati, M. Muccini, D.L. Kaplan, F.G. Omenetto and R. Zamboni, Org. Elec. **12** 1146-1151 (2011).

[21] D. Saravanan, J. Tex. App. Techn. Manag. **5**, 1-18 (2006).

[22] A. Sponner, W. Vater, S. Monajembashi, E. Unger, F. Grosse, and K. Weisshart, Plos One **10**, e998 (2007).

[23] D.J. Little and D.M. Kane, *Conference paper IQEC*, Session **11** (2011).

[24] R.G. Hunsperger, Integrated Optics: Theory and Technology, Springer, New York (1982)

[25] J. Scheuer and A. Yariv, J. Europ. Opt. Soc. **1**, 06007 1-5 (2006).

[26] M.G. Kuzyk, U.C. Paek and C.W. Dirk, Appl. Phys. Lett. **59**, 902-904 (1991).